DOI: 10.1002/chem.200801174

Elusive Trimethyllanthanum: Snapshots of Extensive Methyl Group Degradation in La–Al Heterobimetallic Complexes

Laura C. H. Gerber, Erwan Le Roux, Karl W. Törnroos, and Reiner Anwander*[a]

Abstract: Reactions of $[La(AlMe_4)_3]$ and $[Y(AlMe_4)_3]$ with PMe_3 show that the phosphine can cleave $Ln–CH_3–Al$ linkages, separating $Me_3Al(PMe_3)$. PMe_3 (3 mol equiv) reacts with $[Y(AlMe_4)_3]$ to give $[(YMe_3)_n]$ contaminated with by-products containing phosphorus and aluminum. The La-based analog, $[(LaMe_3)_n]$, is not formed selectively from the reaction of $[La(AlMe_4)_3]$ with PMe_3 or Et_2O, which rather yields insoluble La/Al heterobimetallic products. Three multinuclear La-based clusters were obtained from a reaction of $[La(AlMe_4)_3]$ with PMe_3 (1 equiv) and identified by X-ray structure analyses. Each cluster exhibits extensive methyl group degradation and contains methylene, methine, or carbide moieties. $[La_4Al_8(CH)_4(CH_2)_2(CH_3)_{20}(PMe_3)]$ has a $\{La_4(CH)_4\}$ cuboid core supported by $AlMe_3$, $Me_2AlCH_2AlMe_2$, and PMe_3 ligands. $[La_4Al_8(C)(CH)_2(CH_2)_2(CH_3)_{22}(toluene)]$ also contains a cuboid core, $\{La_3Al(C)(CH)_2(CH_2)\}$, which includes one *exo* cubic lanthanum atom, and is supported by $AlMe_3$, $Me_3AlCH_2AlMe_2$, $(AlMe_4)^-$, and toluene ligands. The lanthanum atoms in $[La_5Al_9(CH)_6(CH_3)_{30}]$ are arranged in a trigonal bipyramidal fashion with (CH) functionalities capping each face. The $\{La_5(CH)_6\}^{3-}$ core is formally balanced by three $AlMe_2^+$ moieties and is additionally supported by six $AlMe_3$ ligands. The unit cell contains two independent La_5 clusters, one with *pseudo*-C_{3h} and the other with *pseudo*-D_3 symmetry, as well as two molecules of the separation co-product $Me_3Al(PMe_3)$.

Keywords: aluminum · bond activation · cluster compounds · lanthanum · methine · methylene

Introduction

Rare-earth metal(III) tetramethylaluminates $[L_xLn(AlMe_4)_y]$ ($y=1$, 2, 3; $x+y=3$, L = monovalent ancillary ligand) are converted efficiently into donor solvent-free complexes $[\{L_xLn(CH_3)_y\}_n]$ by trimethylaluminum separation,[1,2] as evidenced for a number of metallocenes,[1,3] a half-sandwich derivative $[\{(C_5Me_5)LnMe_2\}_3]$ (Ln = Y, Ho),[4] and N-donor-based postmetallocenes.[5,6] We have recently applied this aluminate cleavage reaction protocol to the synthesis of amorphous $[(LnMe_3)_n]$ from $[Ln(AlMe_4)_3]$ (Ln = Y, Lu: Scheme 1).[7,8] We have also shown that C–H bond activation is a viable, albeit low-rate, reaction pathway in mixtures containing both highly reactive $\{Ln–CH_3\}$ moieties and $\{Ln–(CH_3)_x–Al\}$ heterobimetallic linkages.[4,9,10] Accordingly, hydrogen abstraction led to the first structurally authenticated $\{Ln–CH_2\}$[9,10] and {Ln–CH} moieties.[4] Solvent- and alkali metal-free methyl complexes and their degradation products from C–H bond activation can be considered elusive rare-earth metal complexes (Figure 1).[11,12] Herein, we describe the reactivity of $[La(AlMe_4)_3]$ toward neutral donor molecules OEt_2 and PMe_3 involving the formation of

[a] L. C. H. Gerber, Dr. E. Le Roux, Prof. Dr. K. W. Törnroos, Prof. Dr. R. Anwander
Department of Chemistry, University of Bergen
Allégaten 41, 5007 Bergen (Norway)
Fax: (+47) 5558-9490
E-mail: reiner.anwander@kj.uib.no

Supporting information (^1H MAS NMR spectra of $[La(AlMe_4)_3]$ and $[Y(AlMe_4)_3]$, the ^{31}P CP MAS NMR spectrum of $[Y(AlMe_4)_3]$ with excess PMe_3, and the molecular structure of **3c** including cocrystallised coproduct $Me_3Al(PMe_3)$) for this article is available on the WWW under http://dx.doi.org/10.1002/chem.200801174.

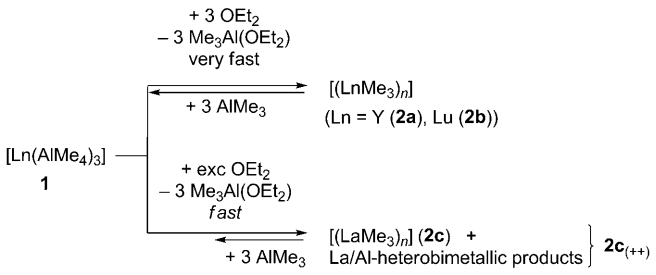

Scheme 1. Reactivity of homoleptic Ln^{III} tetramethylaluminates toward diethyl ether.

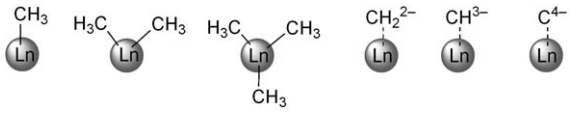

Figure 1. Elusive rare-earth metal(III) C_1 moieties.

discrete mixed methylene/methine/carbide clusters bearing no stabilizing ancillary ligands.

Results and Discussion

Reactivity of [Ln(AlMe$_4$)$_3$] complexes toward diethyl ether: In an attempt to synthesize homoleptic trimethyllanthanum, [La(AlMe$_4$)$_3$] (**1c**)[13] was stirred with a small excess of diethyl ether (Scheme 1). Visually, the precipitation of putative [(LaMe$_3$)$_n$] (**2c**) was significantly slower than in the respective yttrium reaction, producing a pale yellow insoluble powder **2c$_{(++)}$**. Elemental analysis of **2c$_{(++)}$** indicated that AlMe$_3$ was not cleaved completely (Table 1), although the

Table 1. Microanalytical data for precipitates obtained from [Ln(AlMe$_4$)$_3$] cleavage reactions at ambient temperature.

Homoleptic aluminate	Cleavage agent [equiv]	Product	C [wt%]	H [wt%]	Al [wt%][c]
[Y(AlMe$_4$)$_3$] (**1a**)[a]	OEt$_2$ (3)	[(YMe$_3$)$_n$] (**2a**)	26.88	6.51	<0.5
[Lu(AlMe$_4$)$_3$] (**1b**)[a]	OEt$_2$ (3)	[(LuMe$_3$)$_n$] (**2b**)	16.19	3.94	–
[La(AlMe$_4$)$_3$] (**1c**)	OEt$_2$ (exc)	**2c$_{(++)}$**	27.77	5.76	10.20
1a	PMe$_3$ (3)	**2a**	28.74	6.67	2.51
1c	PMe$_3$ (3)	**2c$_{(+)}$**	24.78	4.85	7.66
1c	PMe$_3$ (1)	**3**	27.97	5.41	12.14
		Calculated values			
		1a	41.15	10.36	23.11
		1b	33.03	8.32	18.55
		1c	36.01	9.07	20.22
		2a	26.89	6.77	–
		2b	16.37	4.12	–
		[(LaMe$_3$)$_n$] (**2c**)	19.58	4.93	–
		3a[b]	28.36	6.32	17.57
		3b[b]	32.40	6.40	17.12
		3c[b]	28.36	6.35	17.70

[a] Taken from Ref. [9]. [b] Solvent molecules and coproducts included in the crystalline lattice were not taken into consideration. [c] The Al contents obtained from AAS most probably underestimate the actual contents since the sample preparation was hampered by the extremely violent reaction of such methyl complexes toward aqueous solvents.

^{13}C MAS NMR spectrum revealed only one broad M–CH$_3$ signal at $\delta = 3.9$ ppm (Figure 2A). The presence of diethyl ether in **2c$_{(++)}$** is revealed by two peaks at $\delta = 66.5$ and 15.1 ppm. Neat lanthanum precursor complex **1c** also showed only one ^{13}C signal at $\delta = 10.4$ ppm (Figure 2B), consistent with its solution NMR spectrum.[8b] For comparison, the ^{13}C MAS NMR spectrum of [Y(AlMe$_4$)$_3$] (**1a**) revealed

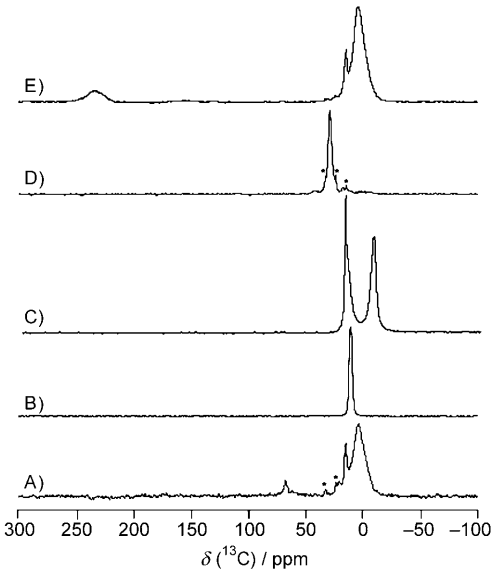

Figure 2. ^{13}C CP MAS NMR spectra of A) [La(AlMe$_4$)$_3$] with excess Et$_2$O (**2c$_{(++)}$**), B) neat [La(AlMe$_4$)$_3$] (**1c**), C) neat [Y(AlMe$_4$)$_3$] (**1a**), D) [Y(AlMe$_4$)$_3$] with excess PMe$_3$ (**2a**), and E) [La(AlMe$_4$)$_3$] with 3 equiv PMe$_3$ (**2c$_{(+)}$**) (*=solvent).

two signals at $\delta \approx -10$ and 18.0 ppm assignable to Y–*C*H$_3$–Al bridging and Al–*C*H$_3$ terminal methyl ligands (Figure 2C).[7] The ^{1}H MAS NMR spectrum of **2c$_{(++)}$** is dominated by two broad resonances centered at $\delta = -0.36$ and 1.2 ppm (**1c**: −0.39 ppm; Figure S1, Supporting Information). Furthermore, whereas [(YMe$_3$)$_n$] (**2a**) is able to undergo the reverse reaction with AlMe$_3$ quantitatively to provide pure **1a**, the La-based products **2c$_{(++)}$** do not yield **1c** purely or quantitatively in the analogous reactions (Scheme 1).

Reactivity of [Ln(AlMe$_4$)$_3$] complexes toward trimethylphosphine: Since the reactions for both La and Y with diethyl ether repeatedly produced noncrystalline insoluble products, we explored the softer donor trimethylphosphine as an aluminate cleavage reagent, as this might slow down the cleavage reaction further in favor of the formation of crystalline Ln-containing products and thermally stable phosphine adduct Me$_3$Al(PMe$_3$).[14,15] Similarly to the oxygen donors diethyl ether and THF, PMe$_3$ reacted with [Y(AlMe$_4$)$_3$] instantaneously to give [(YMe$_3$)$_n$] (**2a**, Scheme 2), the only soluble product visible in the solution NMR spectrum being Me$_3$Al(PMe$_3$).[15] However, the microanalytical data for **2a** cleaved by PMe$_3$ (Table 1: 2.51% Al) show clearly that diethyl ether is a superior cleavage agent for [Y(AlMe$_4$)$_3$]. This is also confirmed by the ^{13}C CP MAS NMR spectrum of **2a** produced with excess of PMe$_3$ which exhibits a small signal at $\delta = 17.2$ ppm (residual PMe$_3$) in addition to the main M–CH$_3$ signal at $\delta = 28.4$ ppm (Figure 2D; compare **2a** cleaved by OEt$_2$: $\delta = 28.5$ ppm).[7] Two peaks at $\delta = 61$ and −52 ppm in the ^{31}P MAS NMR spectrum can also be assigned to the respective residual metal-coordinated phosphine (Figure S2, Supporting Information).

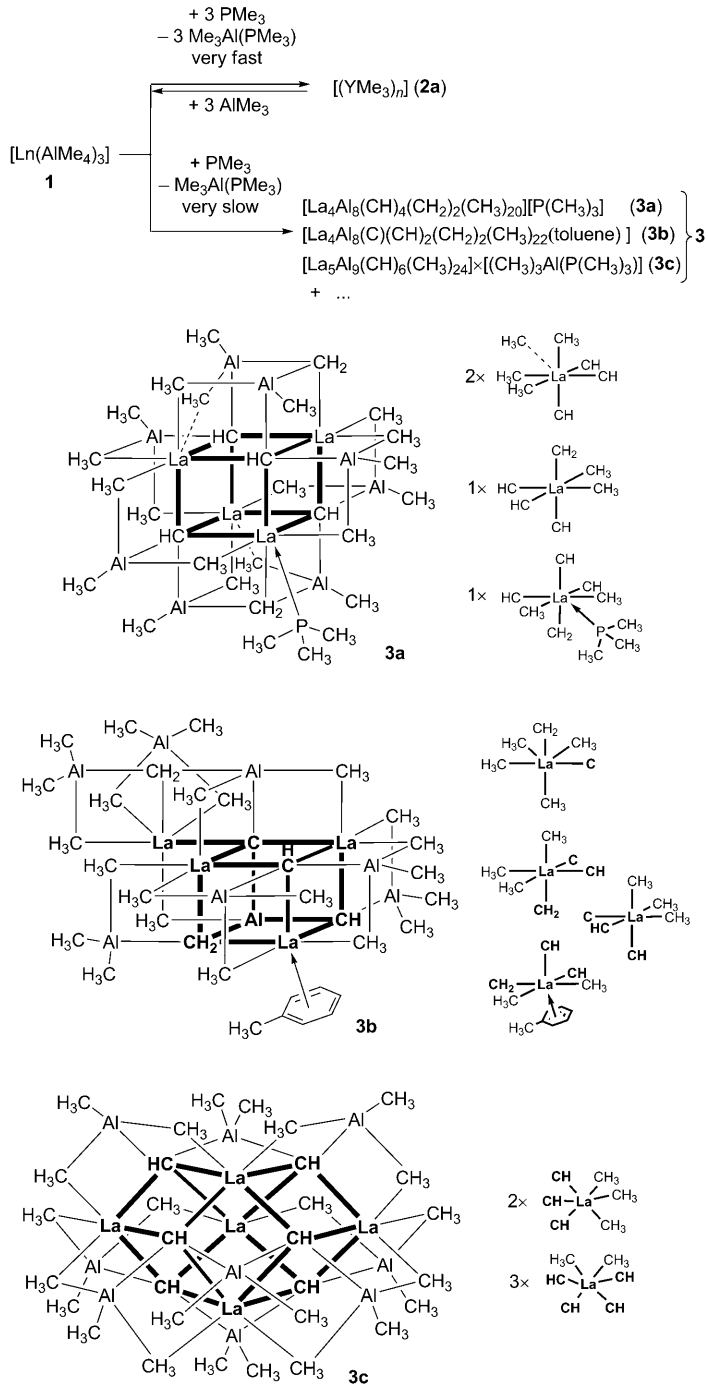

Scheme 2. Reactivity of homoleptic Ln^{III} tetramethylaluminates toward trimethylphosphine: aluminate cleavage versus methyl degradation.

^{13}C MAS NMR spectrum of $\mathbf{2c_{(+)}}$ revealed three signals (Figure 2E) with the broad M–CH_3 resonance showing the same chemical shift ($\delta = 3.9$ ppm) as detected for ether-cleaved $\mathbf{2c_{(++)}}$ (Figure 2A). The ^{13}C signal at $\delta = 14.6$ ppm indicates the presence of trimethylphosphine in $\mathbf{2c_{(+)}}$, and the broad resonance at $\delta = 233.4$ ppm can be assigned to metal-bonded M_3CH methine carbon atoms.[16d] The formation of methine moieties is supported by a broad peak at $\delta = 4.8$ ppm in the ^1H MAS NMR spectrum of $\mathbf{2c_{(+)}}$ (Figure S1, Supporting Information). Examination of the reverse reactions of **3** and $\mathbf{2c_{(+)}}$ with excess $AlMe_3$ showed the presence of $[La(AlMe_4)_3]$ in the ^1H NMR spectra, but this was not isolated pure or in high yields as it is in the analogous reactions with the lutetium and yttrium derivatives **2a** and **2b**.

^1H NMR spectroscopic monitoring of the equimolar reaction of $[La(AlMe_4)_3]$ with PMe_3 over time showed clearly the emergence and disappearance of intermediate species (Figure 3). Initial coordination of the PMe_3 was made evi-

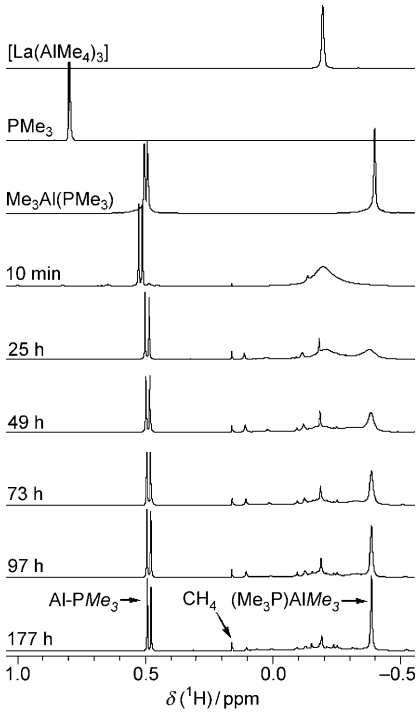

Figure 3. ^1H NMR spectra (400.13 MHz) of $[La(AlMe_4)_3]$ (**1c**) with 1 equiv PMe_3 in C_6D_6 at ambient temperature, the pure starting materials (top two spectra), and independently synthesized $Me_3Al(PMe_3)$.

In contrast, $[La(AlMe_4)_3]$ (**1c**) reacted more slowly (over several hours) with PMe_3 to produce a dark maroon powder $\mathbf{2c_{(+)}}$ (with 3 equiv phosphine; not shown in Scheme 2) or an orange powder **3** with 1 equiv phosphine, which are insoluble in hexane, benzene, or toluene. Based on the carbon content of the elemental analyses, 3 equiv PMe_3 cleaved the homoleptic lanthanum aluminate **1c** more thoroughly than 1 equiv PMe_3 or diethyl ether (Table 1, vide supra). The dent by the shift of proton and phosphorus signals to higher field relative to free trimethylphosphine (uncoordinated PMe_3: ^1H NMR $\delta = 0.79$ ppm, $^{31}P\{H\}$ NMR $\delta = 62$ ppm; metal-coordinated PMe_3: ^1H NMR $\delta = 0.49$ ppm, $^{31}P\{^1H\}$ NMR $\delta = -48.7$ ppm). Over several days the Al-$(CH_3)_3$ resonance of the cleavage co-product $Me_3Al(PMe_3)$ grew and a small methane peak was visible at $\delta = 0.16$ ppm. The tetramethylaluminate signal disappeared almost com-

pletely and a minimum of seven new peaks appeared with even less intensity in the $\delta = 0.1$ to -0.3 ppm region.

Snapshots of methyl group degradation: **formation of methylene, methine, and carbide cluster species**: In accord with the findings from NMR spectroscopic studies (vide supra), slow diffusion of a PMe_3/toluene solution into a [La-$(AlMe_4)_3$]/hexane solution (La/P = 1:1) afforded approximately equal amounts of amorphous and single-crystalline products **3**, over a period of about three weeks. Independent X-ray analyses of three morphologically distinct crystals revealed different nanosized clusters **3a–c** (Scheme 2; Figures 4–6), illustrating the complexity of this reaction. Two

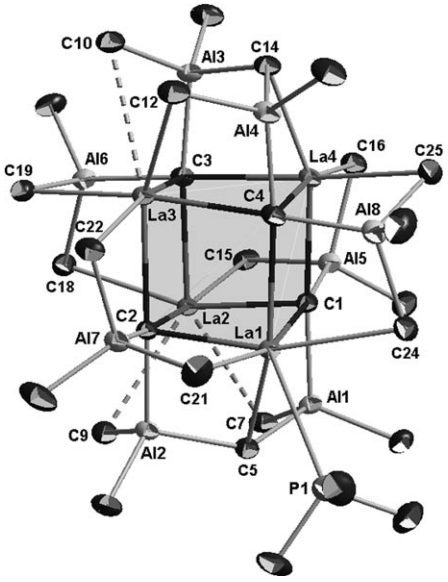

Figure 4. Molecular structure of **3a** (atomic displacement parameters set at the 50% level). Hydrogen atoms are omitted for clarity. Selected bond distances [Å]: La1–C(CH) 2.541(4)–2.794(4), La1–C24(CH_3) 2.800(4), La1–C21(CH_3) 2.913(4), La1–C5(CH_2) 2.629(4), La1–P1 3.3284(11), La2–C(CH) 2.493(4)–2.745(3), La2–C7(CH_3) 3.207(4), La2–C9(CH_3) 3.034(4), La2–C18(CH_3) 2.783(4), La2–C15(CH_3) 2.806(4), La3–C(CH) 2.512(4)–2.714(3), La3–C10(CH_3) 3.257(4), La3–C12(CH_3) 2.992(4), La3–C19(CH_3) 2.744(4), La3–C22(CH_3) 2.744(4), La4–C(CH) 2.530(4)–2.682(4), La4–C14(CH_2) 2.588(4), La4–C16(CH_3) 2.772(4), La4–C25-(CH_3) 2.841(4), Al–C(CH) 2.070(4)–2.128(4), Al–C(CH_2) 2.044(4)–2.102(4), Al–C(terminal CH_3) 1.960(4)–2.038(4), Al–C(bridging CH_3) 2.035(5)–2.060(4).

La_4Al_8 clusters and one La_5Al_9 cluster produced multiple C–H bond activation featuring methylene, methine, or carbide C_1 functionalities.[16,17] The observation of methane and $Me_3Al(PMe_3)$ in the NMR spectra, the irreversibility of the reaction, and the elemental analyses (Table 1) indicate that the few isolated crystals studied by X-ray diffraction must be similar in composition to the major product of the reaction.

The dodecametallic cluster $[La_4Al_8(CH)_4(CH_2)_2(CH_3)_{20}(PMe_3)]$ (**3a**, Figure 4; size $\approx 1.05 \times 1.08 \times 1.35$ nm), which was formed reproducibly, as revealed by two independent X-ray crystallographic studies of crystals from different reac-

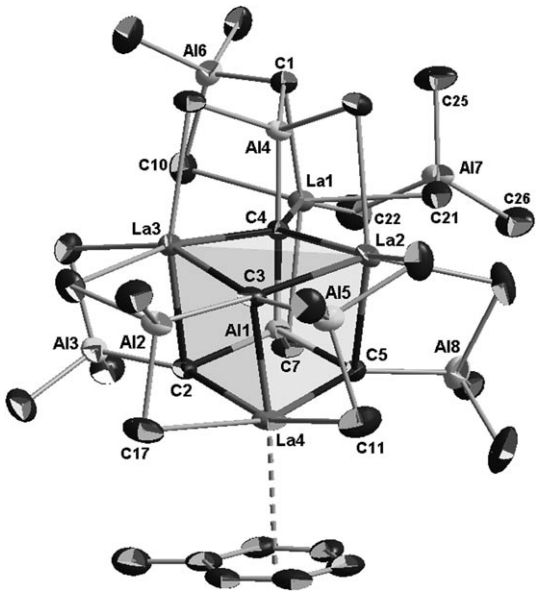

Figure 5. Molecular structure of **3b** (atomic displacement parameters set at the 50% level). Hydrogen atoms are omitted for clarity. Selected bond distances [Å]: La1–C4(carbide) 2.462(6), La1–C1(CH_2) 2.549(7), La1–C10(bridging CH_3) 2.714(8), La1–C7(bridging CH_3) 2.920(7), La1–C21(aluminate) 2.713(8), La1–C22(aluminate) 2.826(7), La2–C4(carbide) 2.475(6), La2–C3(CH) 2.826(7), La2–C5(CH) 2.439(7), La2–C(bridging CH_3) 2.785(9)–2.925(7), La3–C4(carbide) 2.448(6), La3–C2(CH_2) 2.623(7), La3–C3(CH) 2.762(7), La3–C(bridging CH_3) 2.746(7)–2.804(7), La4–C3(CH) 2.529(7), La4–C5(CH) 2.510(7), La4–C2(CH_2) 2.889(7), La4–C17(bridging CH_3) 2.874(9), La4–C11(bridging CH_3) 2.748(9), La4–C_g(toluene) 2.844, Al1–C4 1.975(6), Al1–C7 2.024(7), Al1–C5 2.042(7), Al1–C2 2.063, Al7–C21 2.071(8), Al7–C22 2.064(10), Al7–C25 1.976(8), Al7–C26 1.967(9), Al4–C4 1.979(6), Al–C(bridging CH_3) 2.025(7)–2.082(9), Al–C(terminal CH_3) 1.964(8)–1.989(8), Al–C(CH_2) 2.032(7)–2.111(7).

tions, crystallizes in the monoclinic space group $P2_1/c$ with one molecule of toluene. Cluster **3a** has a cube-like core with lanthanum and methine carbon atoms at alternating apices. Cuboid arrangement of rare-earth metal cations with hydroxide moieties is a common structural motif in the presence of stabilizing chelating ligands such as carboxylates.[18–21] Oxo-,[22] sulfido-/selenido-,[23] and imido-based rare-earth metal cubanes[24] have been characterized by X-ray diffraction previously as well. With the exception of an Er_4S_4 cubane,[23] which is supported by only I^- and THF ligands, the previous cuboid rare-earth metal heteroatom clusters are stabilized by large ancillary ligands. Stabilization of clusters **3a**, **3b**, and **3c** is achieved only by methylaluminum ligands, and weakly coordinating PMe_3 (**3a**) or toluene (**3b**). Moreover, cluster **3a** is the first example of a rare-earth metal-based molecule with a cubane core composed of carbon along with the rare-earth metal.[25,26] Three of the La atoms in **3a** (La2, La3, La4) show a distorted octahedral coordination of carbon atoms with two distinct environments (La2, La3: $3\times$CH, $3\times CH_3$; La4: $3\times$CH, $1\times CH_2$, $2\times CH_3$). La2 and La3 exhibit additional long contacts to C7/C9 (3.207(4)/3.034(4) Å) and C10 (3.257(4) Å), respectively. La1 shows the same carbon connectivity as La4, but is addi-

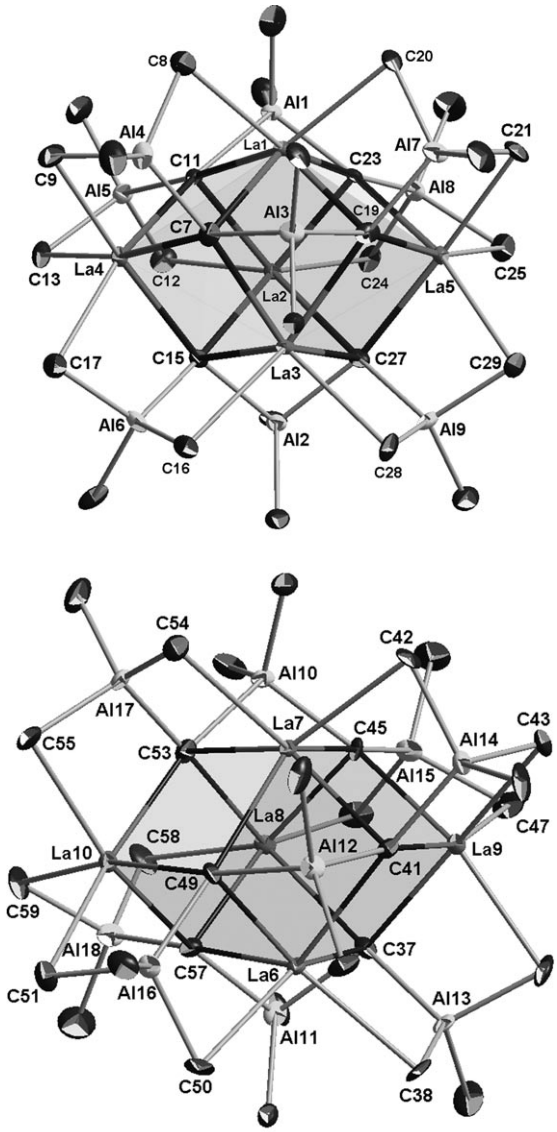

Figure 6. Molecular structure of independent clusters **A** (top) and **B** (bottom) of **3c** (atomic displacement parameters set at the 50% level). Hydrogen atoms are omitted for clarity and co-crystallized $Me_3Al(PMe_3)$ is not shown. Selected bond distances [Å] for **A**: La1–C(CH) 2.538(10)–2.777(9), La1–C8 2.864(10), La1–C20 2.895(10), La2–C(CH) 2.542(9)–2.786(10), La2–C12 2.888(12), La2–C24 2.901(10), La3–C(CH) 2.549(9)–2.768(10), La3–C16 2.901(10), La3–C28 2.868(10), La4–C(CH) 2.588(8)–2.619(10), La4–C(CH_3) 2.742(10)–2.775(11), La5–C(CH) 2.580(10)–2.612(9), La5–C(CH_3) 2.718(10)–2.769(10), Al($AlMe_2^+$)–C(CH) 2.077(11)–2.124(11), Al($AlMe_2^+$)–C(CH_3) 1.955(10)–2.028(12), Al($AlMe_3$)–C(bridging CH_3) 2.020(11)–2.096(11), Al($AlMe_3$)–C(terminal CH_3) 1.939(12)–1.977(11), Al($AlMe_3$)–C(CH) 2.059(10)–2.088(10). For **B**: La6–C(CH) 2.543(10)–2.768(10), La6–C38 2.835(9), La6–C50 2.846(9), La7–C(CH) 2.552(9)–2.766(9), La7–C54 2.822(11), La7–C42 2.860(10), La8–C(CH) 2.551(10)–2.765(11), La8–C46 2.837(10), La8–C58 2.840(10), La9–C(CH) 2.586(10)–2.600(9), La9–C(CH_3) 2.750(11)–2.762(11), La10–C(CH) 2.590(10)–2.601(9), La10–C(CH_3) 2.745(10)–2.762(10), Al($AlMe_2^+$)–C(CH) 2.120(10)–2.150(11), Al($AlMe_2^+$)–C(CH_3) 1.963(10)–2.025(11), Al($AlMe_3$)–C(bridging CH_3) 2.030(12)–2.082(11), Al($AlMe_3$)–C(terminal CH_3) 1.926(12)–2.000(11), Al($AlMe_3$)–C(CH) 2.035(11)–2.084(10).

tionally coordinated by trimethylphosphine. The methine carbon atoms are six-coordinate and have slightly distorted octahedral geometry. In addition to the PMe_3 donor ligand, two distinct types of methylaluminum ligands shield the neutral $\{La_4(CH)_4\}$ cuboid core. Four $AlMe_3$ molecules belt the cube, with an Al atom bonded to each of the four central methine carbon atoms. Two of the methyl groups of each $AlMe_3$ ligand bond to the two different La atoms on each cube face. Two $Me_2AlCH_2AlMe_2$ ligands occupy opposite faces of the cube. The Al–CH_2–Al moieties of the ligands bond to the HC–La–CH of the cube faces. Additionally, a methyl group of one of these ligands also bonds to the second lanthanum of the cube face, thus coordinating to all four atoms of the cube face. Compounds of the type $R_2AlCH_2AlR_2$ ($R=CH(SiMe_3)_2$) have been isolated previously, although not explored as ligands in organometallic chemistry but rather as chelating Lewis acids.[27] The La–C(methyl) bond lengths range from 2.744(4) to 2.992(4) Å, matching those in $[La(AlMe_4)_3]$ (**1c**: 2.696(3)–2.980(3) Å)[8b] and the decametallic La_6Al_4 cluster $[La_6(C_5Me_5)_6(\mu\text{-}Me_3AlMe)_4(\mu_3\text{-}Cl)_2(\mu_2\text{-}Cl)_6]$ (2.771(4)–2.955(3) Å).[25b] The La–C(methine) and La–C(methylene) bond lengths are as short as 2.493(4) and 2.588(4) Å, respectively, the latter comparing to the respective La–CH_2 bond lengths in $[(C_5Me_5)_3La_3(\mu\text{-}Cl)_3(\mu_3\text{-}Cl)(\mu_3\text{-}CH_2)(THF)_3]$ (2.537(3)–2.635(3) Å).[9] The $\{La(PMe_3)\}$ moiety, showing a comparatively long La–P bond (3.328(1) Å),[28] is a rare example of a rare-earth metal trimethylphosphine adduct.[29] In comparison, the La–P bond lengths in eight-coordinate $[La[C(PMe_2)_2(SiMe_3)]_4Li]$ are in the 3.039(2)–3.234(2) Å range,[28a] and the intermolecular La–P bond length in $[(\eta^5\text{-}PC_4Me_4)La(AlMe_4)_2]$ is 3.1962(3) Å.[28b]

Cluster $[La_4Al_8(C)(CH)_2(CH_2)_2(CH_3)_{22}(toluene)]$ (**3b**, Figure 5, size $\approx 0.98\times1.07\times1.40$ nm) crystallizes in the triclinic space group $P\bar{1}$ with three molecules of toluene. Contrary to **3a**, this dodecametallic cluster has a highly distorted cubane core, caused by the displacement of one lanthanum by an aluminum atom and the presence of three distinct carbon C_1 functionalities as apices: one methylene carbon atom, two methine carbon atoms, and one carbide atom. This neutral $\{La_3Al(C)(CH)_2(CH_2)\}$ cuboid core was assigned on the basis of geometrical and charge balance considerations as well as by location of the hydrogen atoms. All four La centers exhibit different coordination environments. La1 ($1\times C$, $1\times CH_2$, $4\times CH_3$), La2 ($1\times C$, $2\times CH$, $3\times CH_3$), and La3 ($1\times C$, $1\times CH$, $1\times CH_2$, $3\times CH_3$) are six-coordinate, whereas La4 attains charge balance through five carbon functionalities ($2\times CH$, $1\times CH_2$, $2\times CH_3$) and steric saturation by the additional η^6-coordination of a toluene molecule.[30] The carbide carbon features a slightly distorted trigonal bipyramidal (tbp) geometry, with three La atoms in the equatorial plane, and two Al atoms in the axial positions (Al1–C4–Al4 = 179.9(4)°). Only slight distortion from tbp geometry was an important criterion to decide in favor of a carbide rather than a methine carbon functionality. This is consistent with the hypercoordinate carbide species $[(Ph_3PAu)_5C][BF_4]$[31] and $[(C_5H_5)Ti(\mu_2\text{-}Me)(\mu_2\text{-}NPPh_3)(\mu_5\text{-}$

C)(μ_2-$AlMe_2$)$_2$($AlMe_2$)($AlMe_3$)],[32] in which a C_{3v}-symmetric and a slightly distorted tbp geometry at the carbide center, respectively, were observed. In complex **3b**, both C3 and C2—a methine and methylene, respectively—have distorted octahedral geometries. The methine carbon C5 is five-coordinate and has distorted square pyramidal geometry, with Al1 (in the cubane core) at the apex. A $(Me_2AlCH_2AlMe_3)^-$ ligand, similar to the neutral $Me_2AlCH_2AlMe_2$ ligands in **3a**, bonds to the carbide carbon through an Al, and three methyl groups and the CH_2 support the La atoms that form the equatorial plane of the carbide carbon. Additionally, the cluster is coordinated by four neutral $AlMe_3$ molecules, one original $(AlMe_4)^-$ ligand which is bonded to the *exo* cuboid lanthanum atom, and one $(CH_3)^-$ ligand bridging the latter with Al1 (in the cubane core). The La–C(methine), La–C(methylene), and La–C(methyl) bond lengths range from 2.439(7) to 2.826(7) Å, 2.549(7) to 2.889(7) Å, and 2.713(7) to 2.920(7) Å, respectively, and hence are comparable to the respective bond lengths in cluster **3a**. The three La–C(carbide) distances (averaging 2.461 Å) are equally short. For comparison, the nearest La–C contacts in binary lanthanum carbides LaC_2 and La_2C_3 are 2.65 and 2.71 Å, respectively,[33] whereas in $[La_{14}(C_2)I_{20}]$ they are as close as 2.345(7) Å.[34,35] Moreover, the La–C(σ) bond length in homoleptic three-coordinate $[La\{CH(SiMe_3)_2\}_3]$ is 2.515(9) Å.[36] The La–C(arene) distances range from 3.136(9) to 3.180(9) Å, matching those in $[La_2(OC_6H_3\text{-}2,6\text{-}i Pr_2)_6]$ (2.978(10)–3.164(9) Å).[37]

The tetradecametallic complex $[La_5Al_9(CH)_6(CH_3)_{30}]$ (**3c**) revealed the highest molecular symmetry, crystallizing in the monoclinic space group C_c, with two independent clusters **A** and **B** and two molecules of $Me_3Al(PMe_3)$ per asymmetric unit (size $\approx 1.07 \times 1.08 \times 1.14$ nm, Figure 6; see also Figure S3 in the Supporting Information). The lanthanum atoms are arranged in a tbp fashion about the center of the molecule, involving two distinct six-coordinate lanthanum environments: La1, La2, La3 ($4\times$CH, $2\times CH_3$); La4, La5 ($3\times$CH, $3\times CH_3$). Six methine moieties, each capping a tbp face, complete the $\{La_5(CH)_6\}^{3-}$ core unit. The methine carbon atoms are each six-coordinate and show La–C distances in the 2.538(10)–2.777(9) Å range. The overall triply negative charge of the core is balanced formally by three $\{AlMe_2\}^+$ fragments which bridge the methine carbon atoms above and below the equatorial plane. Additionally, each methine carbon atom bonds to the aluminum atom of an $AlMe_3$ molecule, two methyl groups of which also bond to one equatorial and one axial lanthanum. The orientation of these $AlMe_3$ ligands determines the different symmetry of the two independent clusters **A** (*pseudo*-C_{3h}) and **B** (*pseudo*-D_3). The co-crystallized $Me_3Al(PMe_3)$ molecules (average P–Al: 2.478 Å)[38] illustrate well how the PMe_3 extracts $AlMe_3$ from the $\{La(Me)_xAlMe_y\}$ aluminate moieties ($x+y=4$).

A possible methyl group degradation pathway: In accord with organoaluminum-promoted (multiple) hydrogen abstraction reactions occurring in early transition metal–methyl complexes,[16,39] we propose the methyl group degradation scenario for $Ln(AlMe_4)_3$-donor (Do) mixtures represented in Scheme 3.

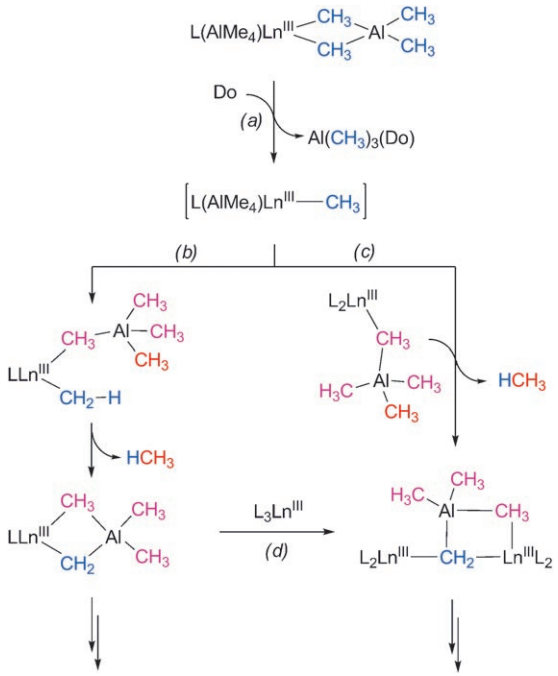

Scheme 3. Hydrogen abstraction from $\{Ln–CH_3\}$ moieties in the presence of alkylaluminate ligands.

Do-induced tetramethylaluminate cleavage (a) involving the formation of highly reactive transient $\{Ln–CH_3\}$ moieties is well documented.[4,5a,9,10] This initial reaction seems to be particularly slow for large rare-earth metal centers (here, lanthanum) and soft donors (here, trimethylphosphine). Moreover, reactions with an Ln aluminate/Do ratio of $\geq$1:1 favor the co-existence of $\{Ln–CH_3\}$ and $\{Ln–(CH_3)_x–AlR_y\}$ moieties ($x+y=4$), which is considered crucial for the occurrence of such C–H bond activation. Next, the strong base $[(CH_3)_xAlR_y]^-$ can abstract a proton from $\{Ln–CH_3\}$ to form methane, trimethylaluminum, and a new $\{Ln–CH_2–M\}$ linkage. Depending on whether the metalation proceeds intra- (b) or intermolecularly ((c), (d); involving ligand redistribution), Tebbe-like "tuck-in" $\{Ln–CH_2–Al\}$ and $\{Ln–CH_2–Ln\}$ linkages are generated, respectively.[5,39] The outcome of these metalation reactions is assumed to be governed by steric factors such as the presence of sterically demanding ligands L.[4,10] Such cleavage/deprotonation sequences continue until either $\{Ln–CH_3\}$ or $\{Ln–(CH_3)_x–AlR_y\}$ moieties are completely consumed, which can also lead to doubly and quadruply deprotonated $\{Ln–CH–M\}$ and $\{Ln–C–M\}$ linkages, respectively. Ether cleavage (Do = OEt_2, THF)[40] and $Me_2P–CH_3$ metalation[41,42] can display alternative reaction pathways in the presence of highly reactive Ln–C(alkyl) bonds, however, such species have not been detected as major degradation products by means of NMR spectroscopy.

Conclusion

In many cases uncontrollable, unpredictable, and serendipitous metal–ligand cluster formation/assembly provides important insights into fundamental chemical processes, whether related to materials science or to catalytic processes. The snapshots of nanosized lanthanum–carbon clusters presented herein document uniquely the high reactivity of {Ln–CH_3} moieties. Unsurprisingly, the high charge density of the hard carbon functionalities CH_2^{2-}, CH^{3-}, and C^{4-} drive cluster formation with the relatively hard La^{3+} cations, thus documenting predominantly ionic interactions. Such extensive degradation of methyl groups may be compared with the deactivation pathways in Ziegler–Natta-type polymerization catalysis.[43,44]

Experimental Section

General procedures: All operations were performed with rigorous exclusion of air and water, by using standard Schlenk, high-vacuum, and glovebox techniques (MBraun MBLab; <1 ppm O_2, <1 ppm H_2O). Hexane, toluene, and diethyl ether were purified with Grubbs columns (MBraun SPS, solvent purification system) and stored in a glovebox. C_6D_6 was obtained from Aldrich, degassed, dried over Na for 24 h, and filtered. PMe_3 solution in toluene and $AlMe_3$ were purchased from Aldrich and used as received. Homoleptic [Ln($AlMe_4$)$_3$] complexes (**1**) were synthesized according to literature methods.[8,13] The solution NMR spectra were recorded by using a Bruker–Biospin-AV500 (5 mm BBO), ^{1}H: $\tilde{\nu}=$ 500.13 Hz; ^{13}C: $\tilde{\nu}=125.77$ MHz, ^{31}P: $\tilde{\nu}=202.5$ MHz), a Bruker–Biospin-AV600 (5 mm cryo probe, ^{1}H: $\tilde{\nu}=600.13$ MHz, ^{13}C: $\tilde{\nu}=150.91$ MHz), or a Bruker-DPX400 (5 mm BBI 1H-BB Z-GRD probe, ^{1}H: $\tilde{\nu}=400.13$ MHz). ^{1}H shifts are referenced to internal solvent resonances and reported in ppm relative to TMS. ^{31}P NMR shifts are reported in ppm relative to 85% H_3PO_4. All solid-state NMR spectra were recorded by using a Bruker 500 MHz Ultrashield Plus equipped with a standard 4 mm double-bearing probe head operating at $\tilde{\nu}=150.91$, 202.45, and 500.13 MHz for ^{13}C, ^{31}P, and ^{1}H, respectively. The samples were placed in ZrO_2 rotors in a glovebox and closed tightly. Compressed air was used for both bearing and driving the rotors. The experimental sample temperature was 298 K with a spin rate of 10 kHz. For ^{1}H MAS NMR, the recycle delay was fixed at 2 s, and eight scans were collected using a 90° pulse excitation of 4.1 μs. For ^{13}C MAS NMR, a typical cross-polarization (CP) sequence was used: 90° rotation of the ^{1}H magnetization (impulsion length, 4.1 μs), then carbon–proton contact for $T_c=4$ ms, and finally recording of the spectrum under high-power decoupling. The delay between transients was fixed at 2 s to allow for complete relaxation of the ^{1}H nuclei, and 38000 scans were made in each experiment. For the ^{31}P CP experiment, the 90° pulse length was 4.1 μs, the recycle delay was 1 s, contact time was set at 1 ms, and 1000 scans were collected. ^{13}C and ^{1}H NMR chemical shifts were referred to adamantane and ^{31}P chemical shifts were referred to 85% H_3PO_4. The ^{13}C and ^{31}P CP MAS fields were similarly line-broadened by 50 Hz and 100 Hz, respectively. IR spectra were recorded by using a Nicolet Impact 410 FTIR spectrometer as Nujol mulls sandwiched between CsI plates. CHN elemental analyses were performed by using an Elementar Vario EL III. Aluminum analyses were performed by using a Perkin–Elmer AAnalyst 300 and give a lower limit of the actual aluminum content since the considerable amounts of sample necessary to conduct the analyses showed a violent reaction toward air and aqueous solvents, inevitably forming small amounts of black materials which were completely insoluble under the prevailing conditions.

CAUTION: All cleavage products and volatiles containing trimethylaluminum react violently if exposed to air.

[Y($AlMe_4$)$_3$] with excess PMe_3 (2a): Complex **1a** (379 mg, 1.08 mmol) was dissolved in hexane ($\approx$7 mL) in a screw-capped vial to make a clear colorless solution. PMe_3 (1.0 M solution in toluene, 6.50 mmol) was added with stirring and a white precipitate formed immediately. The mixture was stirred for 30 min and the precipitate was separated by centrifugation and washed three times with hexane. Hexane fractions were combined and volatiles were removed in vacuo to give pure $AlMe_3(PMe_3)$ as a white powder. Insoluble products were dried in vacuo to give [$(YMe_3)_n$] (**2a**) as a white powder (141 mg, 97%). ^{1}H MAS NMR (500.13 MHz, 25°C): $\delta=1.79$, 1.42, 0.07 ppm (br) (see Figure S1, Supporting Information); ^{13}C MAS NMR (125.77 MHz, 25°C): $\delta=28.4$, 17.2 ppm (see Figure 2); ^{31}P MAS NMR (202.5 MHz, 25°C): $\delta=61$, -52 ppm (see Figure S2 in the Supporting Information).

[La($AlMe_4$)$_3$] with excess Et_2O ($2c_{(++)}$): Complex **1c** (472 mg, 1.18 mmol) was dissolved in hexane ($\approx$7 mL). Et_2O (358 mg, 4.83 mmol) was dissolved in hexane ($\approx$2 mL) and added with stirring to the [La($AlMe_4$)$_3$] solution. The mixture turned opaque white initially and within seconds became a yellow solution with a yellow precipitate. Slow gas evolution was observed. The mixture was stirred for 21 h, during which it turned brown with a brown precipitate. Insoluble products were separated by centrifugation, washed with 4×3 mL hexane, dried in vacuo for several hours to give a brown powder ($2c_{(++)}$, 240 mg), and dried for 4 h under high vacuum. Soluble fractions were filtered, combined, and dried in vacuo to give a brown oil (210 mg). *Insoluble products*: ^{1}H MAS NMR (500.13 MHz, 25°C): $\delta=7.09$ (br), 4.09 (br), 1.02 (br), -0.36 ppm (br) (see Figure S1 in the Supporting Information); ^{13}C MAS NMR (125.77 MHz, 25°C): $\delta=57.6$ (br), 15.1, 3.9 ppm (see Figure 2); IR (Nujol): 2359 (w), 1303 (w), 1191 (w), 1043 (w), 725 (m), 683 cm^{-1} (m). *Soluble products*: ^{1}H NMR (500.13 MHz, 25°C) showed $Me_3Al(OEt_2)$ [$\delta=3.27$ (q, $J=7$ Hz, 4H; CH_2CH_3), 0.66 (t, $J=7$ Hz, 6H; CH_2CH_3), -0.42 ppm (s, 9H; AlMe_3)] as the major product with impurities at $\delta=$ 2.06 (brs), 1.68 (brs), 1.35 (s), -0.10 (s), -0.22 (s), -0.25 (s), -0.32 ppm (m).

The insoluble products (36 mg) were suspended in hexane. $AlMe_3$ (71 mg, 0.98 mmol) was dissolved in hexane and added to $2c_{(++)}$, and the mixture was stirred for 3 h with no visual change. Then more $AlMe_3$ (75 mg, 1.04 mmol) was added and the mixture was stirred overnight. The volatiles were removed in vacuo, and soluble products were extracted with 3×2 mL hexane, centrifuged, and filtered. Volatiles were removed in vacuo from soluble (yellow oil, 39 mg), and insoluble (orange powder, 10 mg) fractions. *Insoluble products*: elemental analysis (%): C 31.09%, H 6.14. *Soluble products*: ^{1}H NMR (500.13 MHz, 25°C) of the yellow oil showed [La($AlMe_4$)$_3$] $\delta=-0.20$ ppm (s) with only trace impurities.

[La($AlMe_4$)$_3$] with 3 equiv PMe_3 ($2c_{(+)}$): Complex **1c** (151 mg, 0.38 mmol) was dissolved in hexane ($\approx$4 mL) and PMe_3 (1.0 M solution in toluene, 1.13 mmol) was added with stirring. The mixture turned brown with a brown precipitate after being stirred overnight. The soluble products were separated by centrifugation and extraction with hexane. Soluble and insoluble products were dried in vacuo. Soluble products were an orange brown solid (68 mg), and insoluble products ($2c_{(+)}$) a dark maroon powder (51 mg). *Insoluble products*: ^{1}H MAS NMR (500.13 MHz, 25°C): $\delta=4.8$ (br), 1.5 (br), 0.18 ppm (br) (see Figure S1 in the Supporting Information); ^{13}C MAS NMR (125.77 MHz, 25°C): $\delta=$ 233.4 (br), 14.6, 3.9 ppm (see Figure 2); IR (Nujol): $\tilde{\nu}=1582$ (w), 1303 (w), 1197 (m), 1068 (w), 954 (w), 721 (m), 671 (s), 608 cm^{-1} (m). *Soluble products*: ^{1}H NMR (500.13 MHz, 25°C): $\delta=0.47$ (d, 9H; $J=6.3$ Hz, $(H_3C)_3PAlMe_3$, -0.38 ppm (s, 9H; $Me_3PAl(CH_3)_3$); ^{31}P{^{1}H} NMR (202.5 MHz, 25°C): δ -48.7 ppm (s, Me_3PAlMe_3).

The brown insoluble products $2c_{(+)}$(41 mg) were suspended in hexane ($\approx$3 mL) and $AlMe_3$ (81 mg, 1.1 mmol), dissolved in hexane ($\approx$1 mL), was added. The mixture was stirred for 3.5 h with no visual change, and the volatiles were removed in vacuo. Soluble products (a yellow oil (6 mg)) were separated by extraction with hexane and centrifugation. Insoluble products formed a red violet solid (36 mg). *Insoluble products*: elemental analysis (%): C 23.27, H 4.39%. *Soluble products*: ^{1}H NMR (500.13 MHz, 25°C) showed [La($AlMe_4$)$_3$] ($\delta=-0.20$ ppm (s)) as the major product with impurities at $\delta=1.88$ (brs), 1.35 (brm), 1.13 (t, $J=$

7.9 Hz), 0.15 (t, $J=8$ Hz), −0.13 (m), −0.18 (s), −0.27 (m), −0.31 ppm (s).

[La(AlMe$_4$)$_3$] with 1 equiv of PMe$_3$ (3): Complex **1c** (151 mg, 0.38 mmol) was dissolved in hexane (≈4 mL) to make a clear colorless solution and PMe$_3$ (1.0 M solution in toluene, 0.38 mmol) was added with stirring. The mixture became an orange solution with an orange precipitate after being stirred overnight. The soluble products were separated by centrifugation and extraction with at least 4×2 mL hexane. Soluble and insoluble products were dried in vacuo. Insoluble products formed a yellow orange powder (**3**, 35 mg) and soluble products formed a yellow oil. *Soluble products*: IR (Nujol): $\tilde{\nu}=1303$ (w), 1202 (m), 1095 (w), 953 (w), 721 (m), 674 (m), 597 (m), 489 cm^{-1} (w). The insoluble products (19 mg) were suspended in hexane (≈3 mL) and excess AlMe$_3$ (50 mg) dissolved in hexane was added. The mixture was stirred for 3.5 h with no visual change, and the volatiles were removed in vacuo. Soluble products were extracted with hexane (4×2 mL), centrifuged, and filtered. Hexane-soluble (yellow oil, 19 mg) and hexane-insoluble (pale orange powder, 7 mg) fractions were dried in vacuo. *Insoluble products*: elemental analysis (%): C 29.79, H 5.57. *Soluble products*: ^{1}H NMR (500.13 MHz, 25 °C) showed La(AlMe$_4$)$_3$ ($\delta=-0.20$ ppm (s)) as the major product with impurities at $\delta=1.12$ (t, $J=8$ Hz), 0.14 (d, $J=8$ Hz), −0.09 (br s), −0.18(s), −0.32 ppm (br s).

Crystallization of clusters 3a–c from [La(AlMe$_4$)$_3$] with PMe$_3$ (1 equiv): Complex **1c** (102 mg, 0.25 mmol) was dissolved in hexane (≈0.5 mL) and transferred to an NMR tube. A small portion of hexane was layered on top. The PMe$_3$ solution (1.0 M in toluene, 0.25 mmol) was added slowly. The tube was left to stand without mixing. After three days a brown precipitate had formed. Several crystals formed over about three weeks.

NMR monitoring of the reaction between [La(AlMe$_4$)$_3$] with PMe$_3$ (1 equiv): Complex **1c** (21 mg, 0.05 mmol) was dissolved in C_6D_6 and transferred to a Youngs NMR tube. PMe$_3$ solution (1.0 M in toluene, 0.05 mmol) was added, then the tube was capped and inverted to mix. ^{1}H NMR spectra were recorded periodically for a week. *Soluble products*: ^{31}P{^{1}H} NMR (202.5 MHz, 25 °C): $\delta=-48.6$ ppm (s, Me$_3$PAlMe$_3$); ^{1}H NMR (500.13 MHz, 25 °C) (see Figure 3, 177 h): $\delta=7.13$ (m, H$_3$C*Ph*), 7.02 (m, H$_3$C*Ph*), 2.11 (s, *H*$_3$CPh), 0.48 (d, $J=6.6$, *Me*$_3$PAlMe$_3$), 0.16 (s, C*H*$_4$), 0.10 (s), 0.06 (br s), 0.00 (br s), −0.10 (s), −0.13 (br s), −0.16 (s), −0.18 (s), −0.20 (s, La(AlMe$_4$)$_3$), −0.21 (br s), −0.24 (s), −0.26 (s), −0.32 (s), −0.39 (s, Me$_3$PAl*Me*$_3$), −0.53 ppm (br s).

Single-crystal X-ray structures: Crystal data and details of the structure determination are presented in Table 2. The crystals were placed in a nylon loop containing Paratone oil (Hampton Research) and mounted directly in the N_2 cold stream (Oxford Cryosystems Series 700) on a Bruker AXS SMART 2 K CCD diffractometer. Data were collected by means of 0.3° ω scans in four orthogonal ϕ settings using Mo$_{K\alpha}$ radiation ($\lambda=0.71073$ Å). A fifth run containing 66 frames was used to assess crystal decay. Data collection was controlled using the SMART program, data integration using SAINT, and structure solution and model refinement using XS and XL, respectively as contained within SHELXTL.[45] All three data sets were corrected for absorption, applying numerical face indexing, and subsequent scaling and incident beam correction as contained in SADABS.[46]

*Compound **3a***: The H atoms on the six-coordinate C atoms all appeared in the difference Fourier map and all refined freely to sensible distances and isotropic displacement values. Subsequently these were refined restraining the C–H distances to be similar within 0.01 Å, and refining a common U_{iso}(H), converging at 0.051(8) Å^2. Noncoordinating methyl groups were refined as rigid and rotating (difference Fourier density optimization) CH$_3$ groups around the respective C–Al bonds. Coordinating methyl groups were refined as rigid pyramidal groups with the same C–H and H–H distances as for the previous refinement, but with the threefold axis of the pyramidal rigid group allowed to be nonparallel with the (H)$_3$C–Al bond axis. The isotropic displacement parameters for the H atoms were set to be 1.5 times that of the pivot C atom. CH$_2$ groups were refined with C–H and H–H distances constrained to be 0.99 and 1.58 Å, respectively. The isotropic displacement parameters for the H atoms were set to be 1.2 times that of the pivot C atom. The aromatic H atoms on the solvent toluene were fixed geometrically with U_{iso}(H) set to be 1.2 times that of the parent carbon atom. The methyl group was refined as a rigid pyramidal group rotating around the C–C bond vector with U_{iso}(H) set to be 1.5 times that of the parent carbon atom.

Table 2. Crystallographic data for clusters **3a**, **3b**, and **3c**.

	3a	**3b**	**3c**
formula	$C_{36}H_{85}Al_8La_4P$	$C_{44.5}H_{92}Al_8La_4$	$C_{36}H_{96}Al_{10}La_5P$
formula wt.	1320.49	1398.66	1524.45
color/habit	pale yellow/ prism	colorless/plate	yellow/flat prism
crystal size [mm]	0.23×0.08×0.08	0.21×0.14×0.07	0.18×0.10×0.02
cryst system	monoclinic	triclinic	monoclinic
space group	$P2_1/c$	$P\bar{1}$	Cc
a [Å]	13.0753(4)	12.0768(3)	12.3155(3)
b [Å]	34.9639(11)	14.7145(4)	21.2845(6)
c [Å]	11.7634(4)	19.3559(5)	46.1441(13)
α [°]	90.00	98.639(1)	90.00
β [°]	93.651(1)	104.293(1)	94.167(1)
γ [°]	90.00	108.740(1)	90.00
V [Å^3]	5366.9(3)	3056.1(2)	12063.7(6)
Z	4	2	8
T [K]	100(2)	100(2)	100(2)
ρ_{calcd} [mg m^{-3}]	1.634	1.520	1.679
μ [mm^{-1}]	3.302	2.880	3.659
F(000)	2592	1382	5936
θ range [°]	1.56/29.52	1.12/26.11	1.00/27.11
index ranges (h,k,l)	$-18\le h\le 18$ $-48\le k\le 48$ $-16\le l\le 16$	$-14\le h\le 14$ $-18\le k\le 18$ $-23\le l\le 23$	$-15\le h\le 15$ $-27\le k\le 27$ $-59\le l\le 59$
rflns integrated	87349	38571	81818
independent rflns/ R_{int}	14975/0.0476	12120/0.0309	26598/0.0516
observed rflns ($I>2\sigma(I)$)	12027	10209	24636
data/restraints/ parameters	14975/72/571	12120/77/659	26598/74/995
$R1$/$wR2$ ($I>2\sigma(I)$)[a]	0.0354/0.0636	0.0493/0.1034	0.0468/0.0958
$R1$/$wR2$ (all data)[a]	0.0518/0.0680	0.0612/0.1099	0.0518/0.0974
GOF (on F^2)[a]	1.094	1.048	1.128
largest diff., peak and hole [e Å^{-3}]	1.56/−0.96	10.99/−4.68	1.73/−2.68

[a] $R1=\Sigma(||F_o|-|F_c||)/\Sigma|F_o|$; $wR2=\{\Sigma[w(F_o^2-F_c^2)^2]/\Sigma[w(F_o^2)^2]\}^{1/2}$; GOF$=\{\Sigma[w(F_o^2-F_c^2)^2]/(n-p)\}^{1/2}$.

*Compound **3b***: The crystal was a pseudo-merohedral twin, complicating data integration and rendering proper absorption correction imprecise. This accounts for the highest residual peak (11 e Å^{-3}, 0.88 Å from La4). The second highest peak was 1.2 e Å^{-3}. The structure contains 2.5 toluene solvent molecules, one coordinated and one sitting on an inversion center, and hence disordered. The H atoms on the six-coordinate C atoms all behave as for **3a** and were therefore refined in the same way, albeit with U_{iso}(H) set to be 1.2 times that of the pivot C atom. All other H atoms were refined as for **3a**.

*Compound **3c***: The structure contains two cluster molecules with different molecular symmetries (C_{3h} and D_3, respectively) and two Me$_3$Al(PMe$_3$) molecules. Of the 12 H atoms predicted on the six-coordinate C atoms, 11 appeared in the difference Fourier maps, also refining sensibly. These were therefore refined as for **3a**, albeit with U_{iso}(H) set to be 1.2 times that of the pivot C atom. The twelfth H atom (H49) showed instability in refinement and its coordinates were therefore fixed at a distance of 1.08 Å, with U_{iso}(H) set to be 1.2 times that of C49. All other H atoms were refined as for **3a**.

CCDC-684927 (**3a**), 684928 (**3b**), and 684329 (**3c**) contain the supplementary crystallographic data for this paper. These data can be obtained free

of charge from the Cambridge Crystallographic Data Centre via www.ccdc.cam.ac.uk/data_request/cif.

Acknowledgements

Financial support from the Norwegian Research Council (project 185206/V30), the Nanoscience@UiB program, and the US–Norway Fulbright Foundation for Educational Exchange (for a Fulbright Fellowship to LCHG) is gratefully acknowledged. We also thank Dr. Yucang Liang for AAS analyses.

[1] J. Holton, M. F. Lappert, D. G. H. Ballard, R. Pearce, J. L. Atwood, W. E. Hunter, *J. Chem. Soc. Dalton Trans.* **1979**, 54.
[2] A. Fischbach, R. Anwander, *Adv. Polym. Sci.* **2006**, *204*, 155.
[3] M. G. Klimpel, J. Eppinger, P. Sirsch, W. Scherer, R. Anwander, *Organometallics* **2002**, *21*, 4021.
[4] a) H. M. Dietrich, H. Grove, K. W. Törnroos, R. Anwander, *J. Am. Chem. Soc.* **2006**, *128*, 1458; b) M. Zimmermann, K. W. Törnroos, R. Anwander, unpublished results.
[5] a) M. Zimmermann, F. Estler, E. Herdtweck, K. W. Törnroos, R. Anwander, *Organometallics* **2007**, *26*, 6029; b) R. Litlabø, M. Niemeyer, K. W. Törnroos, R. Anwander, unpublished results.
[6] C. T. Carver, M. J. Monreal, P. L. Diaconescu, *Organometallics* **2008**, *27*, 363.
[7] H. M. Dietrich, G. Raudaschl-Sieber, R. Anwander, *Angew. Chem.* **2005**, *117*, 5437; *Angew. Chem. Int. Ed.* **2005**, *44*, 5303.
[8] a) W. J. Evans, R. Anwander, J. W. Ziller, *Organometallics* **1995**, *14*, 1107; b) M. Zimmermann, N. Å. Frøystein, A. Fischbach, P. Sirsch, H. M. Dietrich, K. W. Törnroos, E. Herdtweck, R. Anwander, *Chem. Eur. J.* **2007**, *13*, 8784.
[9] H. M. Dietrich, K. W. Törnroos, R. Anwander, *J. Am. Chem. Soc.* **2006**, *128*, 9298.
[10] M. Zimmermann, J. Takats, G. Kiel, K. W. Törnroos, R. Anwander, *Chem. Commun.* **2008**, 612.
[11] For a recent paper on nonsolvated lanthanidocene methyl complexes, see: W. J. Evans, J. M. Perotti, J. W. Ziller, *J. Am. Chem. Soc.* **2005**, *127*, 3894.
[12] For X-ray structurally authenticated scandium dimethyl complexes, see: a) P. G. Hayes, W. E. Piers, L. W. M. Lee, L. K. Knight, M. Parvez, M. R. J. Elsegood, W. Clegg, *Organometallics* **2001**, *20*, 2533.
[13] A. Fischbach, M. G. Klimpel, M. Widenmeyer, E. Herdtweck, W. Scherer, R. Anwander, *Angew. Chem.* **2004**, *116*, 2284; *Angew. Chem. Int. Ed.* **2004**, *43*, 2234.
[14] A. R. Barron, *J. Chem. Soc. Dalton Trans.* **1988**, 3047.
[15] A. Almenningen, L. Fernholt, A. Haaland, J. Weidlein, *J. Organomet. Chem.* **1978**, *145*, 109.
[16] For organoaluminum-assisted multiple hydrogen abstractions in organometallic group 4 and 6 complexes, see: a) P. R. Sharp, S. J. Homes, R. Schrock, M. R. Churchill, H. J. Wasserman, *J. Am. Chem. Soc.* **1981**, *103*, 965; b) A. Herzog, H. W. Roesky, Z. Zak, M. Noltemeyer, *Angew. Chem.* **1994**, *106*, 1035; *Angew. Chem. Int. Ed. Engl.* **1994**, *33*, 967; c) D. W. Stephan, *Organometallics* **2005**, *24*, 2548; d) J. E. Kickham, F. Guérin, D. W. Stephan, *J. Am. Chem. Soc.* **2002**, *124*, 11486.
[17] Thermolysis of $[Ru_3(\mu\text{-}H)_2(MeImCH)(CO)_9]$ (Im = imidazole) gave multiple C–H activation of the *N*-methyl group, producing bridging methylene and methine groups as well as an interstitial carbide ligand in $[Ru_5(\mu_5\text{-}C)(\mu\text{-}H)(\mu\text{-}MeIm)(Me_2Im)(CO)_{13}]$: J. A. Cabeza, I. del Rio, D. Miguel, M. G. Sánchez-Vega, *Angew. Chem.* **2008**, *120*, 1946; *Angew. Chem. Int. Ed.* **2008**, *47*, 1920.
[18] For a review, see: Z. Zheng, *Chem. Commun.* **2001**, 2521.
[19] For a "Eu_{15}" wheel-like core structure showing five vertex-sharing cuboid $Eu_4(\mu_3\text{-}OH)_4]^{8+}$ units: R. Wang, Z. Zheng, T. Jin, R. J. Staples, *Angew. Chem.* **1999**, *111*, 1929; *Angew. Chem. Int. Ed.* **1999**, *38*, 1813.
[20] For supercuboid rare-earth metal hydroxide complexes, see: B.-Q. Ma, D.-S. Zhang, S. Gao, T.-Z. Jin, C.-H. Yan, G.-X. Xu, *Angew. Chem.* **2000**, *112*, 3790; *Angew. Chem. Int. Ed.* **2000**, *39*, 3644.
[21] For a layered network of "Er_{36}" wheels with cubic $\{Er_4(\mu_3\text{-}O)(\mu_3\text{-}OH)_3\}^{7+}$ cluster cores, see: J.-W. Cheng, J. Zhang, S.-T. Zheng, M.-B. Zhang, G.-Y. Yang, *Angew. Chem.* **2006**, *118*, 79; *Angew. Chem. Int. Ed.* **2006**, *45*, 73.
[22] T. Shima, Z. Hou, *J. Am. Chem. Soc.* **2006**, *128*, 8124.
[23] a) A. Kornienko, T. J. Emge, A. Kumar, R. E. Riman, J. G. Brennan, *J. Am. Chem. Soc.* **2005**, *127*, 3501; b) D. Freedman, J. H. Melman, T. J. Emge, J. G. Brennan, *Inorg. Chem.* **1998**, *37*, 4162.
[24] D. Cui, O. Tardif, Z. Hou, *J. Am. Chem. Soc.* **2004**, *126*, 1312.
[25] For other organolanthanide cluster compounds, see: a) R. Anwander, *Angew. Chem.* **1998**, *110*, 619; *Angew. Chem. Int. Ed.* **1998**, *37*, 599; b) H. M. Dietrich, O. Schuster, K. W. Törnroos, R. Anwander, *Angew. Chem.* **2006**, *118*, 4977; *Angew. Chem. Int. Ed.* **2006**, *45*, 4858, and references therein.
[26] For a neutral $[Ba_4Zn_2C_6]$ double cage bearing C–H bond activated $CHSiMe_3$ methylene ligands, see: M. Westerhausen, C. Gückel, P. Mayer, *Angew. Chem.* **2001**, *113*, 2736; *Angew. Chem. Int. Ed.* **2001**, *40*, 2666.
[27] a) M. Layh, W. Uhl, *Polyhedron* **1990**, *9*, 277; b) W. Uhl, F. Hannemann, *J. Organomet. Chem.* **1999**, *579*, 18; c) W. Uhl, F. Hannemann, W. Saak, R. Wartchow, *Eur. J. Inorg. Chem.* **1998**, 921.
[28] a) H. H. Karsch, G. Ferazin, O. Steigelmann, H. Kooijman, W. Hiller, *Angew. Chem.* **1993**, *105*, 1814; *Angew. Chem. Int. Ed. Engl.* **1993**, *32*, 1739; b) E. Le Roux, F. Nief, F. Jaroschik, K. W. Törnroos, R. Anwander, *Dalton Trans.* **2007**, 4866.
[29] For cyclopentadienyl-supported Ln-PMe_3 adducts, see: a) S. Stults, A. Zalkin, *Acta Crystallogr. Sect. A* **1987**, *43*, 430; b) P. J. Shapiro, E. Bunel, W. P. Schaefer, J. E. Bercaw, *Organometallics* **1990**, *9*, 867; c) P. J. Shapiro, W. D. Cotter, W. P. Schaefer, J. A. Labinger, J. E. Bercaw, *J. Am. Chem. Soc.* **1994**, *116*, 4623; d) W. E. Piers, G. Ferguson, J. J. Gallagher, *Inorg. Chem.* **1994**, *33*, 3784; e) S. Arndt, P. Voth, T. P. Spaniol, J. Okuda, *Organometallics* **2000**, *19*, 4690.
[30] G. B. Deacon, Q. Shen, *J. Organomet. Chem.* **1996**, *506*, 1.
[31] F. Scherbaum, A. Grohmann, G. Müller, H. Schmidbaur, *Angew. Chem.* **1989**, *101*, 464; *Angew. Chem. Int. Ed. Engl.* **1989**, *28*, 463.
[32] J. E. Kickham, F. Guerin, J. C. Stewart, D. W. Stephan, *Angew. Chem.* **2000**, *112*, 3406; *Angew. Chem. Int. Ed.* **2000**, *39*, 3263.
[33] M. Atoji, K. Gschneidner, Jr., A. H. Daane, R. E. Rundle, F. H. Spedding, *J. Am. Chem. Soc.* **1958**, *80*, 1804.
[34] H. Mattausch, A. Simon, L. Kienle, C. Hoch, C. Zheng, R. K. Kremer, *Z. Anorg. Allg. Chem.* **2006**, *632*, 1661.
[35] Endohedral lanthanofullerenes can also show short La–C distances: $La_2@C_{80}$, 2.39(3) Å: E. Nishibori, M. Takata, M. Sakata, A. Taninaka, H. Shinohara, *Angew. Chem.* **2001**, *113*, 3086; *Angew. Chem. Int. Ed.* **2001**, *40*, 2998; $[La@C_{82}\{CBr(COOC_2H_5)_2\}]$, 2.520 Å: L. Feng, T. Nakahodo, T. Wakahara, T. Tsuchiya, Y. Maeda, T. Akasaka, T. Kato, E. Horn, K. Yoza, N. Mizorogi, S. Nagase, *J. Am. Chem. Soc.* **2005**, *127*, 17136.
[36] P. B. Hitchcock, M. F. Lappert, R. G. Smith, R. A. Bartlett, P. P. Power, *J. Chem. Soc. Chem. Commun.* **1988**, 1007.
[37] R. J. Butcher, D. L. Clark, S. K. Grumbine, R. L. Vincent-Hollis, B. L. Scott, J. G. Watkin, *Inorg. Chem.* **1995**, *34*, 5468.
[38] Although $AlMe_3(PMe_3)$ is a solid (m.p. 62.5 °C), its structure has been determined only inaccurately by gas-phase electron diffraction (Al–P: 2.53(4) Å) (ref. [13]).
[39] a) F. N. Tebbe, G. W. Parshall, G. S. Reddy, *J. Am. Chem. Soc.* **1978**, *100*, 3611; b) K. C. Ott, E. J. M. deBoer, R. H. Grubbs, *Organometallics* **1984**, *3*, 223.
[40] a) P. B. Hitchcock, S. A. Holmes, M. F. Lappert, S. Tian, *J. Chem. Soc. Chem. Commun.* **1994**, 2691; b) C. Eaborn, P. B. Hitchcock, K. Izod, J. D. Smith, *J. Am. Chem. Soc.* **1994**, *116*, 12071.
[41] a) H. H. Karsch, H. Schmidbaur, *Z. Naturforsch. B* **1977**, *32*, 762; b) L. M. Engelhardt, G. E. Jacobsen, C. L. Raston, A. H. White, *J. Chem. Soc. Chem. Commun.* **1984**, 220.
[42] Trimethylphosphine has previously been employed as a stabilizing donor for highly reactive transition-metal alkyl complexes. For ex-

amples, see: refs. [16a] and [29]; J. E. Kickham, F. Guerin, J. C. Stewart, E. Urbanska, D. W. Stephan, *Organometallics* **2001**, *20*, 1175.
[43] *Ziegler Catalysts* (Eds.: G. Fink, R. Mühlhaupt, H.-H. Brintzinger), Springer-Verlag, Berlin, **1995**.
[44] For an example of a rare-earth metal-based Ziegler catalyst, see: L. Jiang, Y. Zhang, Z. Shen, *Eur. Polym. J.* **1997**, *33*, 577.
[45] a) SMART, Version 5.054, **1999**; b) SAINT, Version 6.45a, **2001**; c) SHELXTL Version 6.12, Bruker AXS Inc., Madison, Wisconsin (USA), **2001**.
[46] SADABS, Version 2008/1, Bruker AXS Inc., Madison, Wisconsin (USA), **2008**.

Received: June 16, 2008
Published online: September 11, 2008

